Evidence of magnetic isotope effects during thermochemical sulfate reduction

Harry Oduro[a,b,1], Brian Harms[a], Herman O. Sintim[c], Alan J. Kaufman[a], George Cody[d], and James Farquhar[a,1]

[a]Department of Geology and Earth System Science Interdisciplinary Center (ESSIC), University of Maryland, College Park, MD 20742; [c]Department of Chemistry and Biochemistry, University of Maryland, College Park, MD 20742; [d]Geophysical Laboratory, Carnegie Institution of Washington, 5251 Broad Branch Road NW, Washington, DC 20015; and [b]Department of Earth, Atmospheric, and Planetary Sciences, Massachusetts Institute of Technology, 77 Massachusetts Avenue, Cambridge, MA 02139-4307

Edited by Mark H. Thiemens, University of California at San Diego, La Jolla, CA, and approved August 23, 2011 (received for review May 24, 2011)

Thermochemical sulfate reduction experiments with simple amino acid and dilute concentrations of sulfate reveal significant degrees of mass-independent sulfur isotope fractionation. Enrichments of up to 13‰ for ^{33}S are attributed to a magnetic isotope effect (MIE) associated with the formation of thiol-disulfide, ion-radical pairs. Observed ^{36}S depletions in products are explained here by classical (mass-dependent) isotope effects and mixing processes. The experimental data contrasts strongly with multiple sulfur isotope trends in Archean samples, which exhibit significant ^{36}S anomalies. These results support an origin other than thermochemical sulfate reduction for the mass-independent signals observed for early Earth samples.

anomalous | sulfur radical | thermolysis | spin-selective | hyperfine coupling

Since the report by Farquhar et al., (1) that significant deviations from the terrestrial fractionation line are observed in samples older than approximately 2.32–2.45 Ga (2, 3), considerable effort has been dedicated to identifying the origin and significance of this signal (4–10). The mass-independent signal in these ancient samples is expressed as variations in both $\Delta^{33}S$ and $\Delta^{36}S$ (1).* Given the observations that gas-phase reactions can produce mass-independent signals for both $\Delta^{33}S$ and $\Delta^{36}S$, the first studies on this subject attributed this ancient signal to photolytic reactions in the early atmosphere. Subsequent studies also pointed out that the mass-independent reactions may also be produced by variations in the spectrum of light that drives atmospheric photolytic reactions (10–12), and other studies speculated that liquid phase reactions involving weakly bound transition states may account for these variations (7, 13).

In a recent report, Watanabe et al. (7) demonstrated that high temperature reduction of sulfate using alanine and glycine as organic substrates caused moderate mass-independent sulfur isotope fractionations. These authors did not identify the origin of the effect, but suggested that it was either a magnetic isotope effect (MIE) (14) or another type of isotope effect accompanying heterogeneous reactions such as adsorption of S-bearing compounds on surfaces of solids (13). Magnetic isotope effects are expressed in rare cases for isotopes with nuclear magnetic moments, like ^{13}C, ^{17}O, ^{29}Si, ^{199}Hg, ^{201}Hg, ^{73}Ge, ^{235}U, and ^{33}S (14, 15, 16). The effect is expressed when the lifetime of a radical pair is sufficient for hyperfine coupling between magnetic nuclei and unpaired electrons to influence interconversions between singlet and triplet states. This coupling in turn changes the proportion of reactive intermediates that can participate in spin-selective reactions. The ^{33}S nucleus has a spin of 3/2 and a magnetic moment of 0.643 nuclear magnetons and has been implicated in at least one well-characterized example of a ^{33}S MIE (14, 17–19). The alternative suggestion relates to a proposal that anomalous isotope effects may be associated with heterogeneous reactions as a result of possible missing vibrational levels involving very weakly bound transition states (13). This proposal has been contested by Balan et al. (20), who argue that no effect exists when a more complete treatment of the reaction mechanisms is undertaken. Uncertainty in ascribing the origin of the effect to an MIE arose because two of their samples possessed $\Delta^{36}S$ that was different from that of the starting materials. Uncertainty, ruling out an MIE (and demonstrating a different type of anomalous isotope effect) also arose because other processes relevant to the complex reaction pathways of thermochemical sulfate reduction (TSR) in their system involve mixing and can generate mass conservation effects (21) that have been shown to produce small variations in $\Delta^{33}S$ and more significant variations in $\Delta^{36}S$ (e.g., $\geq 2‰$ in biological and biogeochemical systems (22, 23).

Here we report results from two sets of high temperature experiments (i.e., flow-reactor and Carius tube experiments) that suggest the observation of ^{33}S anomalies in these reactions are related to a magnetic isotope effect in the reaction products. The mechanistic aspects for the origin of ^{33}S anomalies via disulfide ion-radical pair reaction routes have been proposed through multiple sulfur isotope measurements and ^{33}S electron spin resonance (ESR) spectroscopic evidence (24, 25).

Results and Discussion

The flow through reactor experiments yielded two distinct sulfur products as seen in Table S1 [gaseous H_2S and chromium-reducible sulfur (CRS)] with anomalous ^{33}S enrichments ($\Delta^{33}S$ from $+0.25$ to $+13.1‰$), but no significant change in ^{36}S composition from starting sulfate (Fig. 1 *A* and *B*). In Carius tube experiments, ^{33}S enrichments in acid volatile sulfide (AVS) and CRS products were small to undetectable except when S_8 or $Na_2S_2O_4$ was added (see Table S2) to catalyze reduced sulfur production in the reaction products with no effect to the S-radical chemistry. We speculate that the observed isotope effect originates from ion-radical pair ($RS^{\bullet}H^{+}/RS^{\bullet}SH$) intermediates (24, 26) through the following sequence of reactions:

1. Prolonged heating of glycine (mp = 262 °C) affords three major classes of compounds: (*i*) small neutral molecules, (*ii*) carbon and other carbon-based polymers, and (*iii*) radical intermediates (both heteroatom and carbon-centered radicals) as indicated in Scheme 1 below (27, 28).
2. Sodium sulfate can then be reduced by some of the reducing gases produced in Scheme 1 (e.g., H_2, CO, etc.) to give sodium

Author contributions: H.O. and J.F. designed research; H.O. and J.F. performed research; H.O. and J.F. contributed new reagents/analytic tools; H.O., B.H., H.O.S., A.J.K., G.C., and J.F. analyzed data; and H.O., B.H., H.O.S., and J.F. wrote the paper.

The authors declare no conflict of interest.

This article is a PNAS Direct Submission.

*Here, $\Delta^{33}S = (^{33}S/^{32}S)_{sample}/(^{33}S/^{32}S)_{cdt}\text{-}[(^{34}S/^{32}S)_{sample}/(^{34}S/^{32}S)_{cdt}]^{0.515}$ and $\Delta^{36}S = (^{36}S/^{32}S)_{sample}/(^{36}S/^{32}S)_{cdt}\text{-}[(^{34}S/^{32}S)_{sample}/(^{34}S/^{32}S)_{cdt}]^{1.90}$. Note, this definition is different than that used in ref. 7. The definition used here is consistent with definitions that normalize to a reference array defined by single-step equilibrium isotope exchange reactions and does not impact the conclusions of this study.

[1]To whom correspondence may be addressed. E-mail: hoduro@umd.edu, hoduro@mit.edu, or jfarquha@glue.umd.edu.

This article contains supporting information online at www.pnas.org/lookup/suppl/doi:10.1073/pnas.1108112108/-/DCSupplemental.

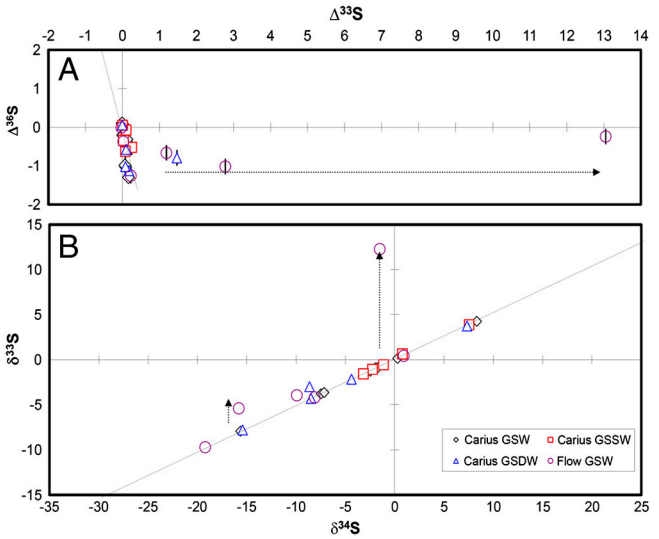

Fig. 1. S-isotope plots of $\Delta^{36}S$ versus $\Delta^{33}S$ (*A*) and $\delta^{33}S$ versus $\delta^{34}S$ (*B*) for Carius tube and flow reactor experiments, abbreviated as GSW (Gly-SO_4^{2-}-H_2O), GSSW (Gly-SO_4^{2-}-S^0-H_2O), and GSDW (Gly-SO_4^{2-}-$S_2O_6^{2-}$-H_2O). Typical mass-dependent arrays are plotted in both panels. Most data follow a tightly constrained, mass-dependent relationship of $\delta^{33}S = 0.515(\pm 0.008) \times \delta^{34}S$ (*B*). Deviations from this array and the $\Delta^{36}S$ versus $\Delta^{33}S$ array are interpreted as magnetic isotope effects. The MIE trends are distinct from sulfur photoexcitation experiments and are not a likely explanation for the Archean sulfur isotope record. Error bars represent 1σ analytical uncertainties of 0.02 and 0.2 for $\Delta^{33}S$ and $\Delta^{36}S$, respectively.

sulfide (**1**, **2**). Trace metal impurities in sodium sulfate can catalyze this reaction. Solid carbon or carbon-based polymers, generated during pyrolysis can also reduce sodium sulfate to sodium sulfide (29, 30) (**3**):

$$Na_2SO_4 + 4CO \rightarrow Na_2S + 4CO_2, \quad [1]$$

$$Na_2SO_4 + 4H_2 \rightarrow Na_2S + 4H_2O, \text{ and} \quad [2]$$

$$Na_2SO_4 + nC \rightarrow Na_2S + CO + CO_2. \quad [3]$$

3. Sodium sulfide in the presence of trace acid and/or water and heat will generate hydrogen sulfide (H_2S) (**4**). The acid/water would come from the H_2O, HCN, and COOH generated during glycine pyrolysis (see Scheme 1) or even from the glycine starting material,

$$Na_2S + 2H\text{-}Y \rightarrow 2NaY + H_2S$$
$$(Y,CN \quad or \quad OH \quad or \quad H_2NCH_2COO^-). \quad [4]$$

4. Hydrogen sulfide can undergo thermolysis (31, 32), which can react with radical intermediates generated during glycine pyrolysis (see Scheme 1) to give thiyl radicals as in [**5**] and [**6**] (33). Note that these reactions are not spin-selective so no ^{33}S anomaly will result,

$$HS\text{-}H + R^{\bullet} \rightarrow HS^{\bullet} + RH \quad R, \text{ carbon-centered radical} \quad [5]$$

$$HS\text{-}H + Y^{\bullet} \rightarrow HS^{\bullet} + HY$$
$$Y, \text{ heteroatom-centered radical.} \quad [6]$$

5a. The thiyl radical ($HS^{\bullet}$) can recombine with other radicals to give neutral, sulfur-containing molecules. Reactions between free radicals (e.g., **7**–**9**) can be spin-selective (34). The absence of measureable sulfur-33 enrichment in the carbon-bound sulfur (Raney Ni fraction) suggests however that this reaction is not the origin of the isotope effect in these experiments,

$$HS^{\bullet} + H^{\bullet} \rightleftharpoons [HS^{\bullet} \quad {}^{\bullet}H]^{T,S} \rightarrow HSH, \quad [7]$$

$$HS^{\bullet} + R^{\bullet} \rightleftharpoons [HS^{\bullet} \quad {}^{\bullet}R]^{T,S} \rightarrow RSH, \text{ and} \quad [8]$$

$$HS^{\bullet} + {}^{\bullet}Y^{\bullet} \rightleftharpoons [HS^{\bullet} \quad {}^{\bullet}Y]^{T,S} \rightarrow YSH$$
$$Y, \text{ heteroatom,} \quad R, \text{ carbon-centered radical.} \quad [9]$$

5b. The products of [**7**], [**8**], and [**9**] can undergo further homolytic cleavage of S-H bonds shown in Scheme 2 to give thiyl radical moieties ($^{\bullet}SH$, $^{\bullet}SY$, and $^{\bullet}SR$). These thiyl radicals have strong reactivity and can also react with other radicals to form polysulfide products via sulfur polymerization (**10**). Such reactions will not produce sulfur-33 enrichments due to strong spin-orbit coupling (see below),

$$RS^{\bullet} + HS^{\bullet} \rightarrow [RS^{\bullet} \quad {}^{\bullet}SH]^{T,S} \rightarrow RS_nH. \quad [10]$$

6. The thiyl radical can also abstract hydrogen from C-H bonds to give carbon-centered radicals. These reactions will not be spin-selective,

$$HS^{\bullet} + H\text{-}R \rightarrow H_2S + R^{\bullet} \text{ and} \quad [11]$$

$$HS^{\bullet} + H\text{-}R \rightarrow RSH + R^{\bullet}. \quad [12]$$

Based on the above sequence of reactions, we propose Scheme 2, which describes the pathway envisioned for production of the observed sulfur-33 enrichments in Cr-reducible sulfur and hydrogen sulfide. We have generalized this sequence of reactions

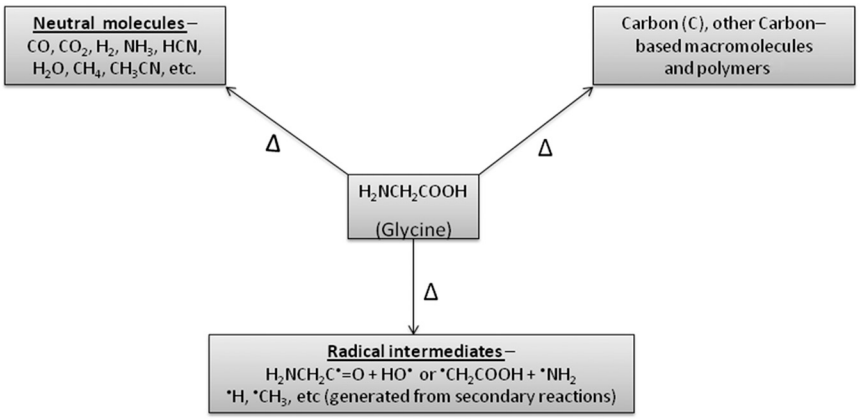

Scheme 1. Pyrolytic decomposition products of glycine. Solid-state NMR and high resolution ESI-MS (in positive mode) confirm the presence of polymers in the reaction mixture.

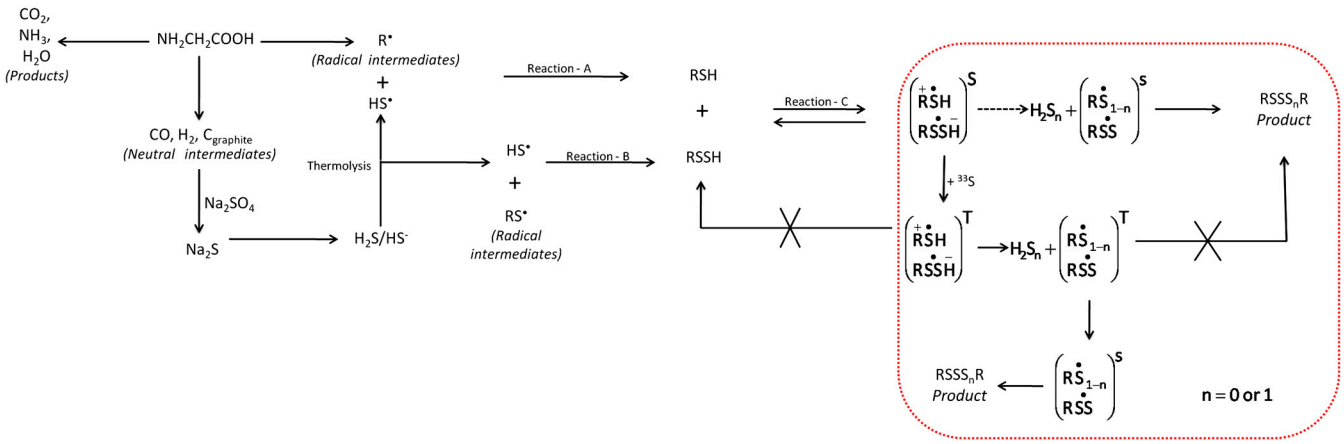

Scheme 2. Proposed ion-radical pair mechanism showing spin evolution between triplet and singlet states during thermochemical sulfate reduction.

by writing it for only R (and not Y and H sulfur bonded radicals). During accidental encounter of free radicals (reactions A and B) in Scheme 2, the statistical distribution of radical pair spin states will be one-fourth singlet and three-fourths triplet states. MIE may occur if this 1:3 proportion is altered by the rapid formation of singlet products upon initial encounter, leaving an excess (>three-fourths) of triplet radical pairs that undergo triplet to singlet conversion. However, these reactions are an unlikely source of MIE because it has been shown that thiyl radicals exhibit strong spin-orbit coupling (35, 36) and therefore are expected to experience rapid spin flipping independent of hyperfine coupling.

We instead suggest that the observation of ^{33}S enrichments in the CRS fraction implicates MIE associated with the formation of polysulfide species [reaction C (Scheme 2) and the subsequent network highlighted in the red box]. We suggest this polymerization reaction of sulfur product is mediated by an ion-radical mechanism similar to that proposed by Buchachenko et al. (26). Here RSH acts as an electron donor to RSSH, forming an ion-radical pair intermediate that is initially in a singlet state. Coulombic attraction inhibits dissociation of the radical pair. Here, the radical pair may either (*i*) reform the original reactants by back electron transfer, (*ii*) slowly lose H_2S_n (where $n = 0$ or 1) in a non-spin-selective manner, or (*iii*) undergo singlet to triplet conversion via ^{33}S hyperfine coupling. Back electron transfer from the triplet state is spin forbidden, and therefore the radical pair must lose H_2S_n to form an $RS^{\bullet}{}_{1-n}/RSS^{\bullet}$ radical pair. Subsequent triplet-singlet conversion allows for the radical pair to combine and thus form a polysulfide ($RSSS_nR$) product. Such products that are formed through the triplet pathway are therefore enriched in ^{33}S. Our mechanism is supported by prior ESR measurements (24, 25), which show that disulfide radicals have ^{33}S hyperfine structure values (~10 G) similar to sulfur nuclei that exhibit MIE. The experimental products also preserve evidence for significant mixing and classical isotope effects that influence $\Delta^{36}S$ in a mass-dependent manner (21, 23), supporting this small anomaly as the cause of ^{36}S variation reported in ref. 7).

The Eschka sulfur and the Cr-reducible sulfur appear to be isotopically fractionated relative to the residual sulfate by two distinct processes. The Eschka sulfur has a mass-dependent ^{34}S enrichment with respect to the starting composition, and the Thode fraction (which include residual sulfate), which is, in turn, ^{34}S-depleted relative to the starting composition. We infer that these observations indicate the principal loss pathway for sulfate is the mass-dependent formation of product sulfur in the Eschka fraction. The Cr-reducible sulfur fraction is ^{33}S-enriched and ^{34}S-depleted, consistent with an MIE following the mechanism described that would yield a smaller secondary product fraction, and a residue with a small ^{33}S-depletion. We interpreted the absence of a measurable fractionation in the Eschka and Raney Ni fractions to reflect dilution of R-SH that formed from non-spin-selective reactions.

Conclusions

We conclude that the origin of MIE is related to sulfur radicals generated by thiyl-mediated thermolysis of H_2S that undergo a rapid ion-radical pair polymerization reaction to form the chromium (II) reducible sulfide product. Because the MIE captured in these TSR experiments principally affects $\Delta^{33}S$ without significantly affecting $\Delta^{36}S$, the relevance of these reactions as an explanation for mass-independent sulfur isotope effects reported from Earth's most ancient rocks (where deviations from mass-dependent arrays are noted for both ^{33}S and ^{36}S) is limited. Moreover, the absence of sulfur isotope mass-independent fractionation in post-Archean organic-rich rocks suggests that TSR is not a widespread source of fractionations in typical sediments and further supports the assertion that the early record does not reflect this chemistry. Thermal reactions have, however, been proposed as a mechanism for formation of sulfur-containing compounds as well as their radical species in a variety of natural systems where organic matter and sulfur radicals are present [e.g., where sulfur radicals control petroleum maturation (37)]. It is possible therefore that sulfur MIE are generated in some settings, and evidence for this effect should be sought.

Experimental Procedure and Methods

Two sets of experiments were undertaken to monitor the products of TSR: (*i*) flow-reactor experiments and (*ii*) Carius tube experiments. Reagent grade sodium sulfate (~0.5 mol/L) and powdered glycine were used in both experiments,

$$SO_4{}^{2-} + 2H_2N\text{-}CH_2\text{-}COOH + H_3O^+{}_{(W)} \xrightarrow[\Delta\text{-Heat}]{} H_2S + 3CO_2 + [CH_2]^{\bullet} + 2NH_3 + 3H_2O. \quad [13]$$

For the flow reactor experiments, glycine and 1.0 mL sodium sulfate solution were added to a reaction flask, matching the stoichiometry of **[13]**, which was heated continuously at approximately 300 °C for 340 h under 15 bubbles/min nitrogen flow. Water lost to evaporation was replenished by injecting 0.5 mL of Milli-Q water through a septum in the reaction flask [three or four times per experiment (Table S1)]. Product hydrogen sulfide carried by the nitrogen flow was isolated by trapping with a Zn-acetate buffer, yielding a white crystalline ZnS precipitate. Solid and liquid residues in the reaction flask were treated by procedures outlined for the Carius tube experiments.

High-purity Pyrex glass Carius tubes (dimension 35.5-cm long, 12-mm outer diameter, ~1.2-mm wall thickness) were loaded with 0.5 mL sodium sulfate solution and glycine to match the

stoichiometry of [**13**]. Two experiments also included sulfur intermediate species, S_8 and $Na_2S_2O_4$ (Table S3), to catalyze the production of sulfide in reaction products. Sample tubes were placed in a stainless steel jacket before being heated in a muffle furnace at temperatures listed in Table S1. After heating, the Carius tubes were chilled with liquid-nitrogen, crack-opened, and zinc acetate added to fix sulfide.

Solid and liquid fractions were isolated from the Carius tubes and placed into a flask for sequential extraction. The sulfur from reaction products were extracted using sequential reaction with 5 N HCl for AVS; Cr(II) acid distillation in ethanol for S-S_n (where $n \geq 1$) fractions (CRS); Raney Ni desulfurization for carbon bonded sulfur; Thode reducible sulfur for sulfate; and Eschka oxidized sulfur for total organic sulfur (methods described in ref. 38). Recovery was incomplete because some material adhered to the Carius tube walls, but upper estimates of the fraction of product Cr-reducible sulfur and Raney Ni reducible sulfur is provided in Table S2. The proportion of Cr-reducible and Raney Ni reducible sulfur relative to Eschka- and Thode-sulfur was determined by the Cline method (39) using a UV-visible double beam (model UVD-3200) scanning spectrophotometer (Labomed Inc.) before converting sulfur into Ag_2S for fluorination in Ni bombs, conversion to SF_6 by heated reaction with F_2, and subsequent S-isotopic analysis in a dual inlet ThermoFinnigan-253 mass spectrometer.

A solid-state NMR was acquired for residual solid fractions after the experiments using a Varian/Chemagnetics Infinity 300 solid-state NMR spectroscopy. High resolution electrospray ionization (ESI)–MS (resolving power 6,000 fwhm) were also taken for liquid fractions in both a positive ion mode using an AccuTOF (JEOL USA, Inc.) TOF–MS. The spray voltage was set to 2.3 kV, and the capillary and orifice temperatures were maintained at 250 °C and 80 °C, respectively. The instrument was typically operated at the following potentials: orifice $1 = 30$ V, orifice $2 = 5$ V, ring lens $= 10$ V. The rf ion guide voltage was generally set to 1,000 V to allow detection of ions greater than $m/z = 100$. Both solid-state NMR and ESI–MS analyses confirm the presence of neutral molecules, complex carbon-based macromolecules, and polymers that were formed through radical condensation reactions.

ACKNOWLEDGMENTS. We thank R. Lawler for his technical assistance and guidance on refining our proposed mechanism. We also thank W. Guo, Y. Li, S.-T. Kim, D. Bentil, and A. Amrani for their comments and discussions that motivated this study. This study was supported by grants from the National Aeronautics and Space Administration Astrobiology Institute, Carnegie Institute of Washington team (to J.F.).

1. Farquhar J, Bao H, Thiemens MH (2000) Atmospheric influence of Earth's earliest sulfur cycle. *Science* 289:756–786.
2. Guo QJ, et al. (2009) Reconstructing Earth's surface oxidation across the Archean–Proterozoic transition. *Geology* 37:399–402.
3. Bekker A, et al. (2004) Dating the rise of atmospheric oxygen. *Nature* 427:117–120.
4. Farquhar J, Savarino J, Airieau S, Thiemens MH (2001) Observation of wavelength sensitive mass-independent sulfur isotope effects during SO_2 photolysis: Implications for the early atmosphere. *J Geophys Res Planets* 106:32829–32839.
5. Pavlov AA, Kasting JF (2002) Mass-independent fractionation of sulfur isotopes in Archean sediments: Strong evidence for an anoxic Archean atmosphere. *Astrobiology* 2:27–41.
6. Zahnle K, Claire M, Catling D (2006) The loss of mass-independent fractionation in sulfur due to a Palaeoproterozoic collapse of atmospheric methane. *Geobiology* 4:271–283.
7. Watanabe Y, Farquhar J, Ohmoto H (2009) Anomalous fractionations of sulfur isotopes during thermochemical sulfate reduction. *Science* 324:370–373.
8. Domagal-Goldman SD, Kasting JF, Johnston DT, Farquhar J (2008) Organic haze, glaciations and multiple sulfur isotopes in the Mid-Archean Era. *Earth Planet Sci Lett* 269:29–40.
9. Halevy I, Johnston DT, Schrag DP (2010) Explaining the structure of the Archean mass-independent sulfur isotope record. *Science* 329:204–207.
10. Lyons JR (2007) Mass-independent fractionation of sulfur isotopes by isotope-selective photodissociation of SO_2. *Geophys Res Lett* 34:L22811.
11. Lyons JR (2009) Atmospherically-derived mass-independent sulfur isotope signatures and incorporation into sediments. *Chem Geol* 267:164–174.
12. Ueno Y, et al. (2009) Geological sulfur isotopes indicate elevated OCS in the Archean atmosphere, solving faint young sun paradox. *Proc Natl Acad Sci USA* 106:14784–14789.
13. Lasaga AC, Otake T, Watanabe Y, Ohmoto H (2008) Anomalous fractionation of sulfur isotopes during heterogeneous reactions. *Earth Planet Sci Lett* 268:225–238.
14. Buchachenko AL (2001) Magnetic isotope effect: Nuclear spin control of chemical reactions. *J Phys Chem A* 105:9995–10011.
15. Bergquist BA, Blum JA (2007) Mass-dependent and -independent fractionation of Hg isotopes by photo-reduction in aquatic systems. *Science* 318:417 420.
16. Ghosh S, Xu Y, Humayun M, Odom AL (2008) Mass-independent fractionation of mercury isotopes in the environment. *Geochem Geophys Geosyst* 9:Q03004.
17. Step EN, Tarasov VF, Buchachenko AL (1990) Magnetic isotope effect. *Nature* 345:25.
18. Turro NJ (1983) Influence of nuclear spin on chemical, reactions: Magnetic isotope and magnetic field effects (A Review). *Proc Natl Acad Sci USA* 80:609–621.
19. Buchachenko AL (2009) *Magnetic Isotope Effect in Chemistry and Biochemistry* (Nova Science Publishers, New York), pp 83–88.
20. Balan E, et al. (2009) Theoretical investigation of the anomalous equilibrium fractionation of multiple sulfur isotopes during adsorption. *Earth Planet Sci Lett* 284:88–93.
21. Farquhar J, Johnston DT, Wing BA (2007) Implications of conservation of mass effects on mass-dependent isotope fractionations: Influence of network structure on sulfur isotope phase space of dissimilatory sulfate reduction. *Geochim Cosmochim Acta* 71:5862–5875.
22. Johnston DT, et al. (2008) Sulfur isotope biogeochemistry of the proterozoic McArthur Basin. *Geochim Cosmochim Acta* 72:4278–4290.
23. Ono S, Wing B, Johnston D, Farquhar J, Rumble D (2006) Mass-dependent fractionation of quadruple stable sulfur isotope system as a new tracer of sulfur biogeochemical cycles. *Geochim Cosmochim Acta* 70:2238–2252.
24. Hadley JH, Jr, Gordy W (1975) Nuclear coupling of ^{33}S and the nature of free radicals in irradiated crystals of cysteine hydrochloride and N-acetyl methionine. *Proc Natl Acad Sci USA* 72:3486–3490.
25. Sullivan PD (1968) Hyperfine splittings from naturally occurring sulfur-33 in electron paramagnetic resonance spectra. *J Am Chem Soc* 90:3618–3622.
26. Buchachenko AL, Kouznetsov DA, Shishkov AV (2004) Spin Biochemistry: Magnetic isotope effects in the reaction of creatine kinase with CH_3HgCl. *J Phys Chem A* 108:707–710.
27. Simmonds PG, Medley EE, Ratcliff MA, Jr, Shulman GP (1972) Thermal decomposition of aliphatic monoamino-monocarboxylic acids. *Anal Chem* 44:2060–2066.
28. Johnson WR, Wang KC (1971) Mechanisms of hydrogen cyanide formation from the pyrolysis of amino acids and related compounds. *J Org Chem* 36:189–192.
29. Cameron JH, Grace TM (1982) Sulfate reduction with carbon is strongly influenced by bed temperature. *Tappi J* 65:84–87.
30. Cameron JH, Grace TM (1983) Kinetic study of sulfate reduction with carbon. *Ind Eng Chem Fundam* 22:486–494.
31. Adesina AA, Meeyoo V, Foulds G (1995) Thermolysis of hydrogen sulphide in an open tubular reactor. *Int J Hydrogen Energy* 20:777–783.
32. Chivers T, Lau C (1985) The thermal decomposition of hydrogen sulfide over alkali metal sulfides and polysulfides. *Int J Hydrogen Energy* 10:21–25.
33. Beare KD, Coote ML (2004) What influences barrier heights in hydrogen abstraction from thiols by carbon-centered radicals? A curve-crossing study. *J Phys Chem A* 108:7211–7221.
34. Buchachenko AL (1995) Magnetic isotope effect. *Theor Exp Chem* 31:118–126.
35. Autrey T, Devadoss C, Sauerwein B, Franz JA, Schuster GB (1995) Solvent cage recombination of 4-benzoylphenylthiyl radicals: Fast intersystem crossing of triplet sulfur-centered radical pairs. *J Phys Chem* 99:869–871.
36. Khudyakov IV, Serebrennikov YA, Turro NJ (1993) Spin-orbit coupling in free-radical reactions: On the way to heavy elements. *Chem Rev* 93:537–570.
37. Lewan MD (1998) Sulfur-radical control on petroleum formation rates. *Nature* 391:164–166.
38. Oduro H, Kamyshny A, Jr, Guo W, Farquhar J (2011) Multiple sulfur isotope analysis of volatile organic sulfur compounds and their sulfonium precursors in coastal marine environments. *Mar Chem* 124:78–89.
39. Cline JD (1969) Spectrophotometric determination of hydrogen sulfide in natural waters. *Limnol Oceanogr* 14:454–458.